Solid Particle Erosion of Heat Treated TNB-V4 at Ambient and Elevated Temperatures

Muhammad Naveed, Richard Stechow, Sebastian Bolz, Katharina Hobusch, Sabine Weiß

Abstract—Solid particle erosion has been identified as a critical wear phenomenon which takes place during operation of aeroengines in dusty environment. The present work discusses the erosion behavior of Ti-44.5Al-6.25Nb-0.8Mo-0.1B alloy (TNB-V4) which finds its application in low pressure gas turbines and can be used for high pressure compressors too. Prior to the erosion tests, the alloy was heat treated to improve the mechanical properties. Afterwards, specimens were eroded at impact angles of 30° and 90° at room and high temperatures (100 °C-400 °C). Volume loss and erosion behavior are studied through gravimetric analysis, whereas erosion mechanisms are characterized through scanning electron microscopy. The results indicate a clear difference in the erosion mechanism for different impact angles. The influence of the test temperature on the erosion behavior of the alloy is also discussed in the present contribution.

Keywords—Solid particle erosion, gamma TiAl, TNB-V4, high temperature erosion.

I. INTRODUCTION

WITH the increase in number of flights in sandy environments, solid particle erosion has been identified as a critical wear phenomenon of aero-engine components. Since World War II, attempts are being made to understand this wear phenomenon and to identify optimal measures to improve the life and performance of the components used in aero engines [1]. Flight in particulate environments lead to drastic degradation of the engine performance due to blunting of the blade edges, reduction of chord and increase of tip clearance [2]. Reports on reduced mean time between overhauls, increased logistic support and associated costs due to component change after particle erosion of components can be found in literature [3]. Measures like coating blades and high efficiency particulate filters have been introduced in order to protect aeroengine components from wear in erosive environments [3], [4]. Moreover, numerous attempts have been made by various researchers in order to model the particle-target interactions during erosion [5]-[10].

Titanium alloys display attractive properties such as low density, high strength, high stiffness and good corrosion, creep, and oxidation resistance up to 750 °C. However, these properties were outweighed by processing and machining difficulties due to the low ductility and fracture toughness at room temperature [11]. Due to advances in manufacturing technologies and a deeper understanding of the microstructure, the deformation mechanisms as well as advances in micro-

Muhammad Naveed is with the Brandenburgische Technische Universität Cottbus-Senftenberg, Department of Engineering, Cottbus, Germany (e-mail: muhammad.naveed@b-tu.de).

alloying, titanium aluminides are now used in high performance turbo chargers for Formula One and sports cars [12]. The usage of this alloy for light weight valves allows for higher rotational speeds which results in a power increase of about 8% [13]. Besides applications in the automotive industry, gamma TiAl alloys are mainly under consideration for the critical components in the high performance gas turbines [14] and are already used in a handful of gas turbines.

Until today TiAl alloys are only used for low pressure turbine blades and in this use case they are limited for the last compressor stages. But TiAl alloys also have the potential to be used as high compressor blades. These blades take the most damage while operation in sandy regions. The use of gamma TiAl alloy in aero engines gives rise to the need of a deeper understanding of its erosion behavior at room and elevated temperatures. The present work highlights the erosion phenomena of Ti-44.5Al-6.25Nb-0.8Mo-0.1B (TNB-V4) alloy at room and high temperatures. Before the specimens were eroded, they were heat treated to obtain optimal structural and mechanical properties. The erosion behavior of the alloys has been evaluated by studying the gravimetric analysis and the volume loss results. Moreover, the erosion mechanisms have been discussed by analyzing the eroded surface and cross-sectional SEM images.

II. MATERIALS AND METHODS

A. Heat Treatment

The heat treatment procedure was chosen based on the results from Bolz et. al. [15] who investigated the microstructure and mechanical properties in different heat treatment conditions of the same β solidifying Ti-44.5Al-6.25Nb-0.8Mo-0.1B (in at.%) alloy. Forging temperature of this alloy lies approximately between 1220 °C to 1280 °C, above the dissolution temperature of the β/B2-phase which reduces the flow stress while forging and below the γ solvus temperature which leads to massive grain growth. The material used for this work was vacuum arc melted twice and hot isostatic pressed at 1260 °C/150bar for 2 hours followed by an extrusion step. A heat treatment process comprising of holding at a temperature of 1270 °C for 1 hour which was followed by air cooling and an aging temperature of 800 °C for 6 hours and furnace cooling. Such a heat treatment process yields the best combination of tensile and creep properties for this alloy [15].

The obtained TNB-V4 consists of a three phase matrix: lamellar colonies consisting of γ –TiAl/α-Ti$_3$Al and globular β-Ti$_2$Al(Nb,Mo) phases (Fig. 1 (a)). These SEM images show a microstructure which is perpendicular to the extrusion

World Academy of Science, Engineering and Technology
International Journal of Materials and Metallurgical Engineering
Vol:10, No:5, 2016

direction. The above discussed heat treatment resulted in a duplex microstructure of the alloy consisting of mainly lamellar colonies with fine lamellar γ grains. Moreover, presence of β/β_0 grains containing γ precipitates at colony boundaries can also be seen (Fig. 1 (b)). Heat treatment at a temperature of 1270 °C leads to a high strength which cannot be achieved at lower heat treatment temperatures. The air cooling enhances the yield stress and reduces the creep strain rate. Moreover, aging at 800 °C results in higher yield stress and work hardening coefficients compared to aging at 1000 °C [15].
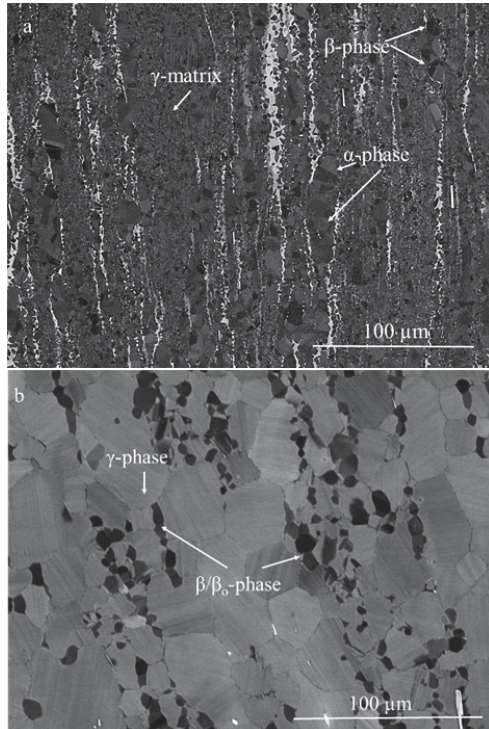

Fig. 1 BSE images of TNB-V4 alloy (a) before heat treatment (b) after heat treatment

B. Experimental Methods

An in-house built high temperature erosion testing rig has been employed for the testing of the specimens (Fig. 2). A compressor is used for providing compressed gas to the series connected heat exchanger. Induction heaters are incorporated within the heat exchanger for the heating of the compressed gas. The compressed hot air is then send to a mixing tube where sand particles from the powder feeder are mixed in. The flow rate of the sand can be controlled by controlling the speed of the rotating plate of the powder feeder (AMT AG, Switzerland). This mixed stream of air and sand particles is then directed towards the specimen holder through a 3 m long tube. This long tube allows a high velocity of the particles at the specimen surface. The specimen temperature of the high temperature jet is measured using an Infratherm IPE 140 pyrometer (IMPAC Infrared GmbH, Germany).

The erosion specimens were cut from an extruded plate of Ti-44.5Al-6.25Nb-0.8Mo-0.1B (in at. %) to a dimension of 30 x 30 x 3 mm and later heat treated as described in Section

II.A. A Tescan Mira II XMH scanning electron microscope (SEM) was used to analyze microstructure before and after the erosion process.

TABLE I
TESTING PARAMETERS USED FOR EROSION TESTS

Erodent	SiO_2
Particle Velocity	~ 180 m/s
Particle Flow Rate	1 g/min
Distance sample to nozzle	25 mm
Angle of incidence	30°,90°
Temperature	25 °C, 100 °C, 200 °C, 300 °C, 400 °C

SiO_2 irregular shaped sand particles (Fig. 3) were used for the testing of the specimens. The average particle size of the SiO_2 particle is estimated between 75-210 µm. The particle velocity was measured through a Laser Doppler Anemometer (LDA) manufactured by TSI (USA). A set of optical lasers with a power of 800 W and a wavelength of 514.5 nm connected to a band pass filter of 20-80 MHz within a signal processor and a photo detector module were used for the measurements. Further details regarding the testing parameters can be found in Table I.

Fig. 2 Schematic representation of the high temperature erosion testing rig
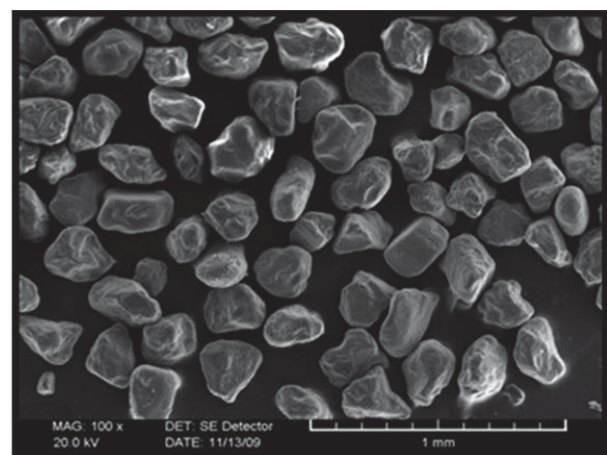

Fig. 3 REM image of the SiO_2 particles used as erodent

World Academy of Science, Engineering and Technology
International Journal of Materials and Metallurgical Engineering
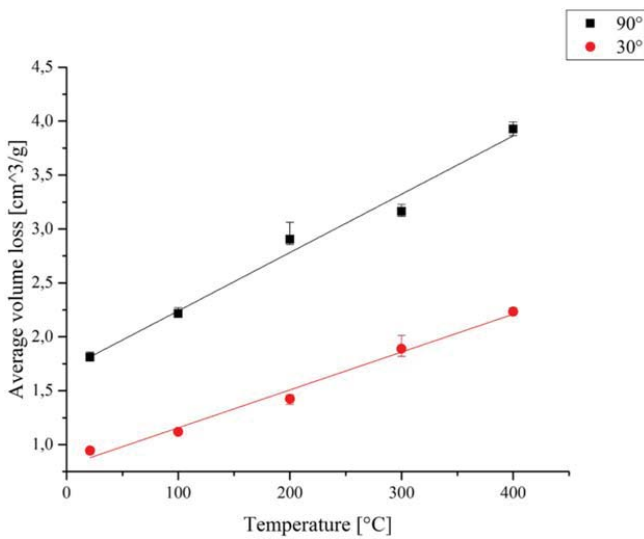Vol:10, No:5, 2016

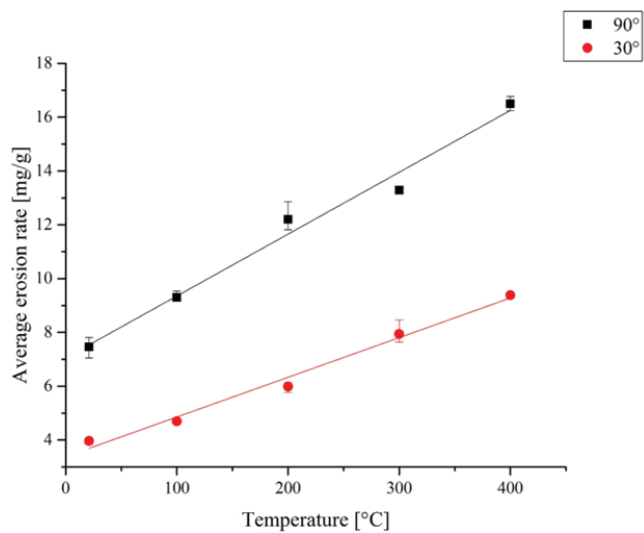## III. RESULTS

A. Erosion Rate and Volume Loss

An analysis on the volume loss and erosion rates of TNB-V4 at oblique and normal impact angles at various temperatures can be found in Fig. 4. The volume loss or erosion rates can be calculated from:

$$\text{Volume Loss} = \frac{\text{Mass loss observed during erosion process}}{\text{density of alloy}} \quad (1)$$

$$\text{Erosion Rate} = \frac{\text{Mass loss observed during erosion process}}{\text{amount of erodent used}} \quad (2)$$

volume loss and erosion rates are seen for normal impact angles in comparison to oblique angles. A linear erosion behavior is depicted with the increase in temperature for both impact angles. Literature reports higher erosion rates at normal angles than at oblique angles for ceramic materials [16]. Hence, a dominant brittle wear would be expected for intermetallic TNB-V4 alloy rather than a metallic ductile behavior. This argument can be supported by studying the loading tests for intermetallics where a brittle fracture is observed for these alloys [15].
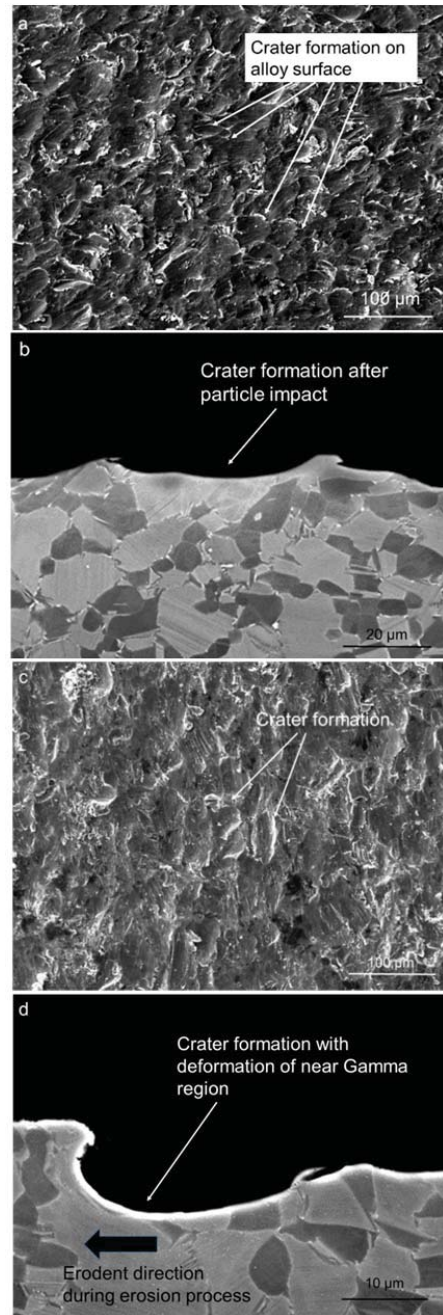

Fig. 5 SEM images of eroded TNB-V4 alloy at 30° impact angle (a), (b) surface (b) cross-section at ambient temperature; (c), (d) surface and cross-section at 400 °C

Fig. 4 (a) Average volume loss, (b) Average erosion rate for 30° and 90° impact angle at the tested temperatures

The volume loss is calculated using a density of 4.2 g/cm³ for TNB-V4. Two measurements have been performed for each test temperature. Higher temperatures lead to an increase in erosion rates and a larger volume loss. Moreover, higher

World Academy of Science, Engineering and Technology
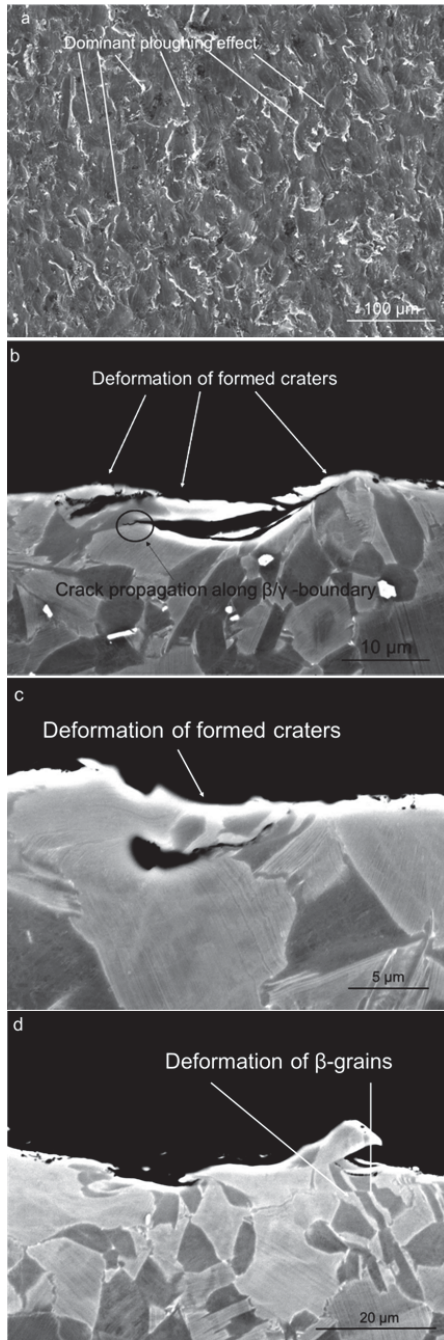International Journal of Materials and Metallurgical Engineering
Vol:10, No:5, 2016

Fig. 6 SEM images of eroded TNB-V4 alloy at 90° impact angle (a) surface (b)-(d) cross-sections at ambient temperature

A microstructural analysis of the eroded TNB-V4 alloy at various conditions can be seen in Fig. 5. Even though the erosion rates predict a ceramic behavior due to high erosion rates at normal angle, a more metallic nature of the alloy can be seen from the alloy surface as a dominant cutting effect was identified for oblique angles at ambient temperatures (Fig. 5 (a)). Moreover, formation of lips/craters (Figs. 5 (a) and (b)) can be seen on the alloy surface. The presence of ploughing effects can also be observed but it is minimal in comparison to the observed cutting effects in some regions. Erosion at elevated temperature (400 °C) still shows cutting processes as an active wear phenomenon (Fig. 5 (c)). The density of the cutting marks on the alloy surface is comparatively lower than in the case of ambient temperature. On the other hand, an increase in the size with lower lip formations can be seen. Cross-sectional SEM images of TNB-V4 alloy also show a crack generation due to the cutting mechanisms at room temperature and 30° impact angle. High deformation in the near gamma regions lead to bending of lamella's in the erodent's impact direction. Such a behavior is not dominantly present for β-phase in the alloy. Cross-sections for erosion tests at 400 °C show large size craters (~ 35 μm) formed in the direction of the erosion impact (Fig. 5 (d)). The mechanical properties like hardness and Elastic Modulus, Yield strength, fracture toughness etc. also play a vital role during the erosion process [17], [18]. A comparison of hardness measurements of all the three phases shows a limited deformation of the α/α_2-phase [19]. Additionally, the lamellar structures exhibit a high anisotropy in ductility, whereas deformation of $\gamma-$ and β/β_0-phase determines the deformation of the alloy at low temperatures [20]-[22]. However, the lamellar structure occupies more than two-third of the available microstructure of TNB-V4 in this case. Therefore, the surface deformation is manly based on the deformability of this lamellar structure, which is controlled by the orientation of lamella to force transmission. If the lamellar structures are orientated under 0° or 90°, the deformability is low and under 45° the deformability is high. The deformability is low if the lamellar structures are oriented at angles of 0° or 90° and high in case of 45° orientation. Therefore, depending on impact angle and lamellar orientation, the lamellar structures tends to deform by cracking for angles of 0° and 90° and by sliding or bending for angles of 45°. Moreover, microploughing dents are observed for the normal angles at ambient temperature and at 400 °C (Figs. 7 (a) and 8 (a)). Microploughing is a process which takes place due to the sliding of the erodent on the alloy surface [23]. Finnie [24] reported ploughing as a material removal phenomenon at shallow impact angles whereas Kameyama and Komotori [25] found that ploughing can also be seen due to shot peening effects at normal angles. A similar behavior was observed in the tested alloy where microploughing can be identified at both normal and oblique angles. Cross-sectional SEM images at ambient temperature show that the formed craters bend due to repetitive particle impacts (Figs. 6 (b) and (c)). It is assumed that these repetitive impacts would lead to further crack propagation resulting in material removal from the alloy surface. A particular example of such a crack propagation can be seen in Fig. 6 (b) at the β/γ grain boundaries. Deformation in the β-grains can also be seen on the alloy surface (Fig. 6 (d)). Hence at normal angles, strong deformation behavior in β-grains along with γ-lamellas could be identified.

Erosion tests at elevated temperature lead to high erosion rates and volume loss. This can be attributed to the deterioration of mechanical properties (hardness, young modulus and strength) of the alloy at high temperatures. A decrease in yield strength for Ti-25Al-10Nb-3V-Mo alloy with the increasing temperature has been postulated by Howard

World Academy of Science, Engineering and Technology
International Journal of Materials and Metallurgical Engineering
Vol:10, No:5, 2016

[26]. Similarly, Bolz et. al. also observed a yield strength of 720 MPa at room temperature, whereas it decreased to 570 MPa at 700 °C [15]. This decrease in yield strength would lead to extensive plastic deformation beneath the eroded surface during the erosion process, whereby the energy required for material removal would be lowered [27]. A similar theory has been suggested by Hutchings [7], where he correlated repetitive particle impact with high strains obtained through cyclic loading. An accumulation of plastic deformation takes place on the alloys surface layers due to this repeated loading. Hutchings defined critical strain as an important parameter that influences the solid particle erosion process. When the accumulation of plastic deformation exceeds the critical strain of the material, removal of material takes place as it detaches from the alloy surface. SEM investigations of cross-sections at 400 °C show formation of larger craters compared to the ambient temperature. A 45 µm crater can be seen on the alloy surface after erosion at 400 °C (Fig. 7 (b)). As previously seen, deformation of formed craters (Figs. 7 (b)-(d)) can be observed after repetitive particle impacts.
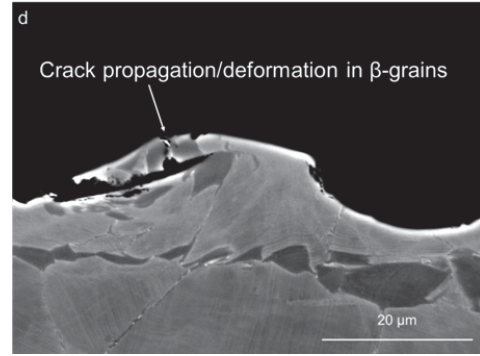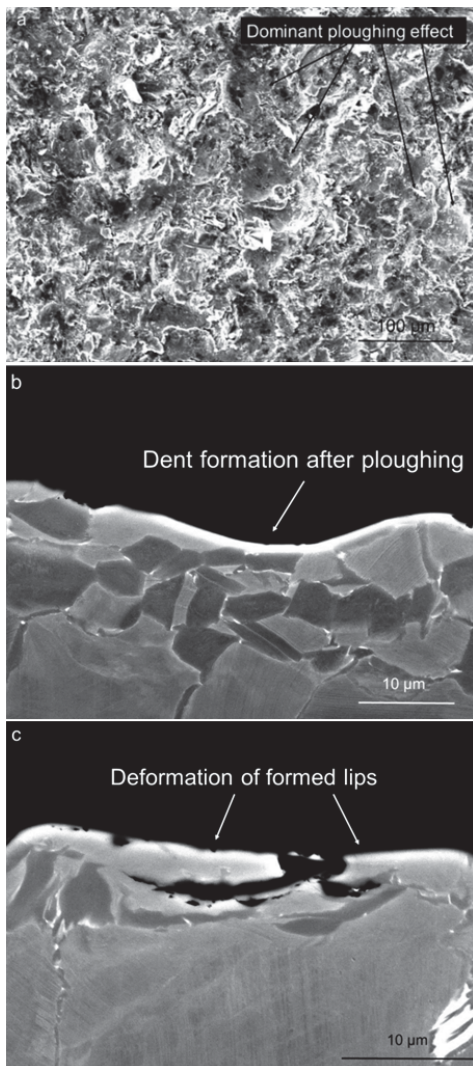

Fig. 7 SEM images of eroded TNB-V4 alloy at 90° impact angle (a) surface (b), (c), (d) cross-section at 400 °C

Another reason for the change of the material removal phenomenon for intermetallics at high temperatures (up to 400 °C) has been defined by Peters and Leyens [28]. They reported on the strain ageing of γ-TiAl alloys during repeated load. At a temperature range of 450 to 650 K, the Le-Chatelier effect is reported. Strain ageing at this temperature range leads to segregation of defects and towards available dislocations leading to brittleness of the alloy.

IV. CONCLUSIONS

A study on the solid particle erosion of Ti-44.5Al-6.25Nb-0.8Mo-0.1B alloy (TNB-V4) has been discussed in the present work. The tests were performed at oblique and normal angles at various temperatures. Following are the main outcomes of the study:

- An increase in volume loss and erosion rates was observed for increasing testing temperatures.
- Erosion rates at oblique angles were higher than at normal angles, indicating brittle behavior of the alloy
- Cutting and ploughing were observed as the main wear phenomenon.
- The microstructure of the alloy controls the wear properties of the alloy.
- Erosion at oblique angles leads to more damage of γ-lamellar phase whereas damage of both γ- and β-phase is seen at normal angle.

A detailed study on the role of individual phases on the deformation during erosion can lead to a better understanding of the erosion process, which will be discussed in the upcoming research papers. Moreover, due to the limited testing capacity, erosion tests were only possible up to a temperature of 400 °C. Erosion testing at real operational condition temperatures between 600 °C - 800 °C would allow for a better design of TiAl alloys. A very limited number of researches have been done in the past to better understand the erosion behavior of intermetallic TiAl alloys. Hence, a need to study the erosion process through variation in testing parameters (shape of erodent, velocity, flow rate etc.) might be useful for further research.

World Academy of Science, Engineering and Technology
International Journal of Materials and Metallurgical Engineering
Vol:10, No:5, 2016

REFERENCES

[1] Tabakoff, W., *High temperature erosion resistance of coatings use in gas turbine engines.* Surface and coatings technology, 1992(52): p. 65-79.

[2] Hamed, A., W. Tabakoff, and R. Wenglarz, *Erosion and deposition in turbomachinery.* Journal of Propulsion and Power, 2006. 22(2): p. 350-360.

[3] Walt, J.P.v.d. and A. Nurick, *Erosion of dust-filtered helicopter turbine engines, Part 1: Basic theoritical considerations* Journal of Aircraft, 1995. 32(1): p. 106-111.

[4] Tabakoff, W., *Protectection of coated superalloys from erosion in turbomachinery and other systems exposed to particulate flows.* Wear, 1999. 233-238(1999): p. 200-208.

[5] Finnie, I. and D.H. McFadden, *Velocity dependence of the erosion of ductile metals by solid particles at low angles of incidence* Wear, 1978. 48: p. 181-190.

[6] Hutchings, I.M. *Some comments on the theoretical treatment of erosive particle impacts.* in *5th International Conference on Erosion by Solid and Liquid.* 1979. Cambridge University, England.

[7] Hutchings, I.M., *Mechanism of the erosion of metals by solid particles,* in *Erosion: Prevention and Useful Applications,* W.F. Edler, Editor. 1979. p. 59-76.

[8] Hutchings, I.M., *A model for the erosion of metals by spherical particles at normal incidence.* Wear, 1980. 70: p. 269-281.

[9] Foley, T. and A. Levy, *Erosion of heat-treated steels.* Wear, 1983. 91(1): p. 45-64.

[10] Shewmon, P. and G. Sundararajan, *The erosion of metals.* Annual Review of Materials Science, 1983. 13: p. 301-318.

[11] Kothari, K., R. Radhakrishnan, and N.M. Wereley, *Advances in gamma titanium aluminides and their manufacturing techniques.* Progress in Aerospace Sciences, 2012. 55: p. 1-16.

[12] Clemens, H., *Intermetallic Materials for Automotive and Aero-engine Applications.* BHM Berg- und Hüttenmännische Monatshefte, 2008. 153(9): p. 337-341.

[13] Chandley, D., *Use of gamma titanium aluminide for automotive engine valves.* 2000, Metal Casting Technology: Italy

[14] Bartolotta, P.A. and D.L. Krause, *Titanium Aluminium Applications in the High Speed Civil Transport.* 1999, NASA: USA.

[15] Bolz, S., et al., *Microstructure and mechanical properties of a forged β-solidifying γ TiAl alloy in different heat treatment conditions.* Intermetallics, 2015. 58: p. 71-83.

[16] Neilson, J.H. and A. Gilchrist, *Erosion by a stream of solid particles.* Wear, 1967. II: p. 111-122.

[17] Bitter, J.G.A., *A study of erosion phenomena (Part II).* Wear, 1962(6): p. 169-190.

[18] Finnie, I., Wolak, and Kabil, *Erosion of surfaces by solid particles.* Journal of materials, 1967. 2(3): p. 682-700.

[19] Schloffer, M., et al., *Microstructure development and hardness of a powder metallurgical multi phase γ-TiAl based alloy.* Intermetallics, 2012. 22: p. 231-240.

[20] Appel, F. and R. Wagner, *Microstructure and deformation of two-phase γ-titanium aluminides.* Materials Science and Engineering: R: Reports, 1998. 22(5): p. 187-268.

[21] Yamaguchi, M., H. Inui, and K. Ito, *High-temperature structural intermetallics.* Acta Materialia, 2000. 48(1): p. 307-322.

[22] Yamaguchi, M. and Y. Umakoshi, *The deformation behaviour of intermetallic superlattice compounds.* Progress in Materials Science, 1990. 34(1): p. 1-148.

[23] Kameyama, Y. and J. Komotori, *Effect of micro ploughing during fine particle peening process on the microstructure of metallic materials.* Journal of Materials Processing Technology, 2009. 209(20): p. 6146-6155.

[24] Finnie, I., *Erosion of surfaces by solid paricles.* Wear, 1960. 3: p. 253-258.

[25] Kameyama, Y. and J. Komotori, *Tribological properties of structural steel modified by fine particle bombardment (FPB) and diamond-like carbon hybrid surface treatment.* Wear, 2007. 263(7–12): p. 1354-1363.

[26] Howard, R.L., *The erosion of titanium aluminide intermetallic alloys,* in *Department of Materials Engineering.* 1995, University of Cape Town.

[27] Levin, B.F., et al., *Modeling solid-particle erosion of ductile alloys.* Metallurgical and Materials Transactions A, 1999. 30(7): p. 1763-1774.

[28] Terlinde, G., T. Witulski, and G. Fischer, *Schmieden von Titan,* in *Titan und Titanlegierungen.* 2007, Wiley-VCH Verlag GmbH & Co. KGaA. p. 303-320.